Adsorption (2014) 20:61–75
DOI 10.1007/s10450-013-9549-9

Gas phase SMB for propane/propylene separation using enhanced 13X zeolite beads

M. C. Campo · M. C. Baptista · A. M. Ribeiro · A. Ferreira · J. C. Santos · C. Lutz · J. M. Loureiro · A. E. Rodrigues

Received: 15 January 2013 / Accepted: 26 April 2013 / Published online: 10 May 2013

Abstract A gas phase simulated moving bed technology using improved 13X zeolite beads and isobutane as desorbent is assessed for the separation of propane/propylene. Adsorption equilibrium (via gravimetric method) and dynamics (via breakthrough curves) were determined in order to validate the mathematical model used to describe the adsorption process. Simulation results have shown that it is possible to separate propylene from a mixture with propane using gas phase SMB technology. The results indicate that high purity propylene (99.99 % desorbent free basis) can be recovered up to 99.96 % with a productivity of 17.6 mol kg^{-1} h^{-1}, with propane being also recovered at high levels (99.98 %) and high purity (99.89 % desorbent free basis). Comparing the SMB simulation results obtained for this new 13X zeolite beads with those obtained with a commercial 13X zeolite characterized elsewhere, it was found that the productivity of the process was raised by 25 %, with half desorbent consumption.

M. C. Campo · M. C. Baptista · A. M. Ribeiro (✉) · A. Ferreira · J. C. Santos · J. M. Loureiro · A. E. Rodrigues (✉)
Laboratory of Separation and Reaction Engineering, Associate Laboratory LSRE/LCM, Department of Chemical Engineering, Faculty of Engineering, University of Porto, Rua Dr. Roberto Frias s/n, Porto 4200–465, Portugal
e-mail: apeixoto@fe.up.pt

A. E. Rodrigues
e-mail: arodrig@fe.up.pt

Present Address:
M. C. Campo · J. C. Santos
Jacobs Engineering Group Inc., Haven 190, Noorderlaan 127, 2030 Antwerp, Belgium

C. Lutz
Service Adsorption, Groupement de Recherches de Lacq, Arkema France, BP 34, 64170 Lacq, France

Keywords 13X zeolite · Gas phase SMB · Propylene/propane separation · Adsorption · Simulation

List of symbols

Variables

a_p	Particle specific area (m^{-1})
Bi_i	Mass biot number of component i, $\left(Bi_i = \frac{a_p k_f R_p^2}{\varepsilon_p 15 D_{p,i}}\right)$ (–)
$C_{g,i}$	Gas phase concentration of component i (mol m^{-3})
$C_{g,T}$	Total gas phase concentration (mol m^{-3})
C_p	Gas mixture molar specific heat at constant pressure (J mol^{-1} K^{-1})
$\overline{C_{p,i}}$	Average concentration of component i in the macropores (mol m^{-3})
$\hat{C}_{ps}$	Particle specific heat at constant pressure (per mass unit) (J kg^{-1} K^{-1})
$\overline{C_{p,T}}$	Average total concentration in the macropores (mol m^{-3})
$\hat{C}_{pw}$	Wall specific heat at constant pressure (per mass unit) (J kg^{-1} K^{-1})
C_v	Gas mixture molar specific heat at constant volume (J mol^{-1} K^{-1})
$C_{v,ads,i}$	Molar specific heat of component i in the adsorbed phase at constant volume (J mol^{-1} K^{-1})
$C_{v,i}$	Molar specific heat of component i at constant volume (J mol^{-1} K^{-1})
d_p	Adsorbent particle diameter (m)
d_{wi}	Internal bed diameter (m)
D_{ax}	Axial dispersion coefficient (m^2 s^{-1})
$D_{c,i}$	Crystal diffusivity of component i (m^2 s^{-1})
$D_{p,i}$	Macropore diffusivity of component i (m^2 s^{-1})

h_f Film heat transfer coefficient between the gas and particle (J s^{-1} m^{-2} K^{-1})
h_w Film heat transfer coefficient between the gas and wall (J s^{-1} m^{-2} K^{-1})
k_f Film mass transfer coefficient (m s^{-1})
nc Number of components
P Pressure (Pa)
$\overline{q_i}$ Average adsorbed phase concentration of component i (mol kg^{-1})
q_i^* Adsorbed concentration of component i in equilibrium with $\overline{C_{p,i}}$ (mol kg^{-1})
r_c Crystal radius (m)
R_g Ideal gas constant (J mol^{-1} K^{-1})
R_p Adsorbent particle radius (m)
t Time (s)
t_s Switching time (s)
T_g Bulk phase temperature (K)
T_p Solid temperature (K)
T_w Wall temperature (K)
T_∞ Ambient temperature (K)
u_0 Superficial velocity (m s^{-1})
U Overall heat transfer coefficient (J s^{-1} m^{-2} K^{-1})
y_i Gas phase molar fraction of component i (–)
z Axial position (m)

Greek letters

α_w Ratio of the internal surface area to the volume of the column wall (m^{-1})
$\alpha_{w\ell}$ Ratio of the log mean surface to the volume of column wall (m^{-1})
$(\Delta H_{ads})_i$ Heat of adsorption of component i (J mol^{-1})
ε Bed porosity (–)
ε_p Particle porosity (–)
γ Ratio between the fluid and solid interstitial velocities, $\left(\gamma_i = \frac{u_i}{u_s}\right)$ (–)
λ Heat axial dispersion coefficient (J s^{-1} m^{-1} K^{-1})
μ Bulk gas mixture viscosity (kg m^{-1} s^{-1})
ρ Bulk gas mixture density (kg m^{-3})
ρ_b Bed density (kg m^{-3})
ρ_p Particle density (kg m^{-3})
ρ_w Wall density (kg m^{-3})

1 Introduction

Propylene is one of the most important feed stocks in the chemical industry, namely for the production of polypropylene, among other chemicals. However, the worldwide demand of propylene is greater than its production (Aitani 2006). Indeed propylene manufacture is limited by the production of other products like ethylene via steam cracking or gasoline from fluid catalytic cracking (Aitani 2006). In 2010, Global Business Intelligence Research issued a report entitled "Polypropylene Market to 2020—Propylene Supply Shortages to Restrict Industry Expansion", where they predict propylene feedstock shortage due to a shifting from a heavy feedstock (crude oil) to a light feedstock (natural gas) in the ethylene production (GBI-Research 2010). Ethylene production from lighter feedstock is cheaper and hence is more profitable. But due to this, the amount of propylene produced is lower. Propylene is mainly a by-product from cracking of heavy liquids, and cracking of light feedstock produces dramatically less propylene by-product. Therefore, propylene supply shortages can be expected due to the increasing demand by the polypropylene industry (GBI-Research 2010). Last year, Nexant® reported that U.S. propylene supply decreased due to the recent discovery of U.S. shale gas reserves, leading to current increase in ethane cracking, which is expected to increase more in coming years (CHEMSYSTEMS 2012). They also stated that propylene production in the United States from ethylene crackers declined, and, for the first time in 20 years, propylene prices were higher than ethylene prices. The subsequent propylene production/demand gap is expected to increase in the coming years. Liquefied petroleum gas cracking in Europe will have a similar impact, although the displacement of hydrocarbons liquids will not be nearly as pronounced as in North America. Hence, shortages of propylene feedstock are likely in these two regions, which will suffer impact in other regions through rise in the propylene commodity price (CHEMSYSTEMS 2012). Therefore, the recovery of propylene from mixtures with propane has come to high commercial significance.

The purity specifications for propylene production depend on its final use: (a) polymer-grade propylene (ca. 99.5 %) for the production of polypropylene and copolymers, (b) chemical-grade propylene (ca. 95 %), used in the production of several synthetic organic chemicals or (c) refinery-grade propylene (ca. 65 %), to produce alkylate (Bryan 2004).

Since propane and propylene present very similar volatilities, separating these two components by a distillation process is difficult and energy consuming. As a consequence, alternative technologies capable of separating propylene from propane in a more effective and less costly way have been investigated. Adsorption based processes, selectively adsorbing some of the components, came up as an attractive and reliable solution. Very promising results have been achieved by cyclic adsorption processes, particularly with pressure or vacuum swing adsorption (PSA/VSA), yielding propylene at a high purity level, but with relatively low recovery. This technology can be simple (Jarvelin and Fair 1993; Cheng and Wilson 2001a, b;

Rodrigues et al. 2008) or hybrid, if combined with distillation (Ghosh et al. 1993). In addition, gas phase simulated moving bed (SMB) (Rodrigues et al. 2008) appeared as a promising and competitive alternative to produce high purity propylene from mixtures with propane, with higher recovery and productivity. The gas-phase SMB process should replace the high energy demanding propane/propylene separation and be followed by two easier downstream separations (propane/desorbent and propylene/desorbent).

The SMB technology was introduced fifty years ago and has been mostly employed to liquid phase separations in a very large scale production of the petrochemical industry (Broughton and Gerhold 1961; Ruthven and Ching 1989). The SMB technology promotes a continuous and counter-current contact between the solid and the gas phase. The main benefit of such process is a more efficient use of the adsorbent which results in a highly efficient mass transfer. Gas-phase SMB operation would combine the previously mentioned high mass transfer due to the counter-current operation with the reduced non-selective holdup of the gas-phase (Mota et al. 2007). However, gas-phase SMB processes have not been used in industry up to now. Even though, a combination of fluidized bed/true moving bed (TMB) is employed for removal of volatile organic compounds/solvents from air—Purasiv HR process (Yang 1987). In the 90′s, vapour-phase separations of xylene isomers and linear/branched paraffins started to be studied by GC-SMB at laboratory scale (open loop—no recycle between zone IV and I) (Storti et al. 1992; Baciocchi et al. 1996; Mazzotti et al. 1996). It was reported on those studies that units with a small number of columns (eight) can achieve high separation performance indices, such as high purity products, recovery, and productivity. In more recent years, other gas phase SMB separations emerged in the literature: methane/carbon dioxide (Mota and Esteves 2007; Mota et al. 2007), oxygen/argon (Rothchild 2001), production of nitrogen from air (Rothchild 2001), hydrogen/helium (Abe et al. 2002), deuterium/helium (Abe et al. 2002), and propylene/propane (Cheng and Wilson 2001a; Rao et al. 2005; Gomes et al. 2009). A configuration similar to the five-zone "clean-in-place" liquid-phase SMB configurations was proposed recently by Kostroski et al., using a new configuration gas-phase SMB/PSA (Kostroski and Wankat 2008). In this configuration desorbent is added at low pressure to the extract-producing zone, while high pressure desorbent can be optionally added to the active loop of the train at high pressure, leading to a four-zone or five-zone SMB/PSA process (Kostroski and Wankat 2008). However, in these configurations some degrees of freedom are lost due to the removal of the regeneration zone from the active loop (Kostroski and Wankat 2008).

The principle of SMB technology lies on the choice of an adequate adsorbent-desorbent couple (Lamia et al. 2008). The adsorbent should be capable of selectively adsorbing propane and propylene and the desorbent should be able to displace them from the solid. Moreover, the desorbent should be easily separated from propane and propylene and have, ideally, intermediate adsorption equilibrium to the ones of propane and propylene. For the cyclic separation processes for the propane/propylene system, several hydrocarbons have been pointed out by Lamia (2008) as potential desorbents, i.e. isobutane, butene-1, *n*-butane, *n*-pentane, neopentane, cyclopropane, cyclobutene and cyclopentane. Isobutane is a good candidate since it follows both criteria mentioned above. Once isobutane is selected, the downstream separations can be two distillation columns (propane/isobutane and propylene/isobutane boiling points differ significantly), identical to the already existing depropanizers or preferentially with two PSA units using MIL-100(Fe) as recently published by Plaza et al.(2012b) As for solid adsorbents, the ones used for the abovementioned gas-phase system are: silica gel, activated carbons, carbon molecular sieves, zeolites 4A and 13X, chemical adsorbents with π-complexation metals (i.e. copper or silver ions), and most recently, MOFs (Chen and Yang 1995; Rege et al. 1998; da Silva and Rodrigues 1999; Zhu et al. 1999; da Silva and Rodrigues 2001a, b; Rege and Yang 2002; Grande et al. 2005; Wagener et al. 2006; Ruthven and Reyes 2007; Wagener et al. 2007; Lamia et al. 2009; Grande et al. 2010a; Jorge et al. 2010; Yoon et al. 2010a, b; Ferreira et al. 2011; van den Bergh et al. 2011; Plaza et al. 2012a).

Lamia et al. (2007) reported the use of a 13X zeolite and isobutane as adsorbent and desorbent, respectively, and presented adsorption equilibrium and dynamics data. Granato et al. (2010) has performed molecular simulation studies listing possible desorbents for the problem mixture under study on zeolite 13X. However publications on this topic are still very scarce and a lot of research is still to be done, especially regarding the design of SMB.

New and improved zeolite 13X beads have been chosen as the adsorbent for this study. Adsorption equilibrium data of propane and propylene for this material were recently reported (Campo et al. 2013) but adsorption equilibrium data of isobutane has been determined in the framework of this paper, at 323, 373 and 423 K, up to 350 kPa. Breakthrough curves of pure isobutane, pseudo-binary and pseudo-ternary curves, namely those of isobutane displacing mixtures of propane and propylene, have been determined. A mathematical model has also been used to predict these curves and a good match was found, corroborating the assumptions made and the model itself. Fixed bed experiments confirmed isobutane as an eligible desorbent for this system; isobutane was able to displace propane and

propylene from 13X. Furthermore, the mathematical model was implemented in a simulator prepared using gPROMS® interface and the separation region for the adsorptive separation of propane/propylene by a SMB has been determined.

2 Experimental

2.1 Materials

The adsorbent considered for this study is a 13X zeolite provided by CECA (Service Adsorption, Groupement de Recherches de Lacq, ARKEMA FRANCE, BP 34, F- 64170 Lacq, France) as beads with an average diameter of 0.7 mm. The improvement on the adsorbent results mainly from a simultaneous reduction of the binder content in the agglomerates at a level close to 11 % and from a better management of the dehydration process during the manufacturing of the zeolite. The gases used in this work, i.e. propane, propylene and isobutane were supplied by Air Liquide.

2.2 Adsorption equilibrium measurements

The adsorption equilibrium isotherms of isobutane were determined using the gravimetric method and accounting for buoyancy effects (Ferreira et al. 2011). The experiments were performed in a magnetic suspension balance from Rubotherm (metal version with 2×10^{-5} g precision) at 323, 373 and 423 K, up to 350 kPa. Prior to adsorption measurements, the sample was degassed under vacuum at 423 K until no mass loss was observed.

The adsorption equilibrium curves of propane and propylene on this adsorbent are reported elsewhere (Campo et al. 2013).

2.3 Fixed bed experiments

The adsorption dynamics of propane, propylene and isobutane on shaped 13X zeolite was studied through breakthrough curves using a fixed-bed unit described elsewhere (da Silva and Rodrigues 2001b).

Very briefly, the fixed bed adsorption unit used within this work is composed of one stainless steel column unit (filled up with the adsorbent under study) placed inside an air-forced convection oven (Termolab) allowing to work in the temperature range of 303–673 K. The pressure of the system is controlled using a back pressure regulator (Bronkhorst High Tech) from 0.1 to 5 bar and vacuum is obtained with a diaphragm pump from KNF (model N813.3 ANE). Individual gas streams or mixtures are fed to the system using up to three mass flow controllers from Teledyne. The column is 2.1 cm in inner diameter and 84 cm height. The temperature history inside the bed can be followed by three K type thermocouples which are mounted at 16.2, 41.2 and 66.2 cm from the bottom end; the bottom and middle thermocouples are placed approximately at the center of the solid bed, while top thermocouple is located at a point near the wall. The unit is automatically controlled by Advantech Genie software.

The composition of the outlet stream is analyzed on-line by a gas chromatograph Chrompack CP9001 equipped with an alumina capillary column (J&W Scientific) and a Flame Ionization Detector, FID. Ethane is used as internal standard.

The fixed bed and adsorbent characteristics are summarized in Tables 1 and 2.

3 Description of the gas phase SMB system

The SMB unit can be considered as a closed system, composed of a given number of columns connected in series with manifolds or ports. The fluid flows continuously through the columns, while the counter current movement of the solid, which occurs in the TMB, is simulated by periodically shifting the inlets and outlets in the direction of the fluid flow, as show in the Fig. 1.

The SMB unit (see the scheme in Fig. 1) has two inlets (feed and desorbent) and two outlets (extract and raffinate), which are at a specified position at a given time (represented by the black arrows). The ports divide the unit into four sections with different roles (Johannsen 2007):

- *Section I* starting at the desorbent inlet and ending at the extract port, this section has the purpose of ensuring that the adsorbent reaches the beginning of the next section cleaned, which means that all compounds should desorb—regeneration zone.
- *Section II* begins at the extract port and ends at the feed inlet. In this section the more retained species should adsorb and the less retained species should flow with the fluid. The contamination of the extract stream with undesired species should be avoided, by establishing convenient switching times.
- *Section III* this section begins at the feed inlet and ends at the raffinate port. As in the previous section, the more retained species should adsorb and the less retained species should flow with the fluid. The more

Table 1 Fixed bed dimensions

Bed length (m)	8.4×10^{-1}
Bed diameter (m)	2.15×10^{-2}
Bed porosity	0.5

Table 2 Properties of the adsorbent

Adsorbent	13X
Adsorbent shape	Spheres
Particle radius (m)	3.5×10^{-4}
Particle density (kg m^{-3})	1300
Particle porosity	0.39
Crystal diameter (m)	2.8×10^{-6}

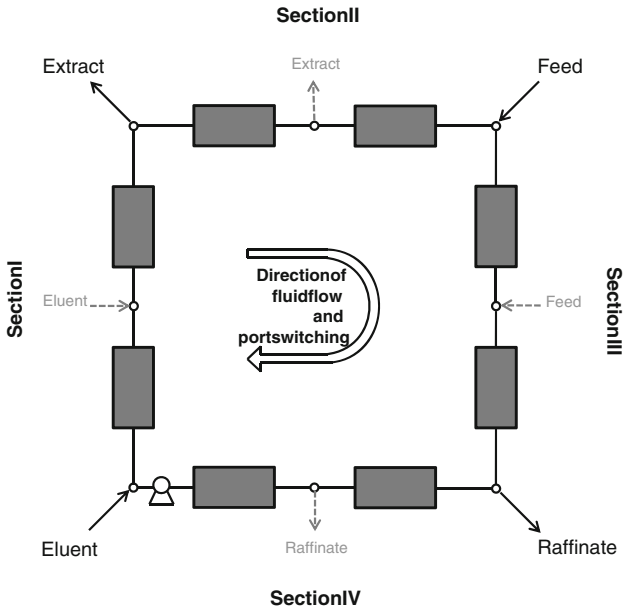

Fig. 1 Scheme of an SMB process

retained species should be prevented from reaching the end of the section and contaminate the raffinate.

– *Section IV* starts at the raffinate port and ends before the desorbent inlet. In this section the eluent should be cleaned, that is, the species should not break through the section.

After a set period of time (switching time), the positions of the ports move one column in the direction of the fluid flow (represented by the gray dashed lines). This shifting of the ports leads to a cyclic steady state (CSS) operation of the SMB unit.

A 2–2–2–2 (8 beds) configuration has been considered for this study. The SMB bed dimensions and operating conditions are reported in Table 3. The adsorbent parameters were previously presented in Table 2.

4 Model and simulation

A mathematical model to describe the adsorption dynamics in a fixed bed has been developed and validated experimentally, through breakthrough curves. This model includes mass, energy, and momentum balances, representing a non-isothermal, non-diluted and multicomponent adsorption system. This same model was used to simulate the SMB unit for the purification of propylene from mixtures with propane, using isobutane as eluent over the selected adsorbent. The main assumptions of the model are the following:

Table 3 SMB bed dimensions

Bed length (m)	9×10^{-2}
Bed diameter (m)	2.15×10^{-2}
Bed porosity	0.5
Switching time (s)	70
Feed temperature (K)	373
Feed pressure (kPa)	150
Feed composition	C_3H_8: 0.25
	C_3H_6: 0.75

- Ideal gas behavior;
- Plug flow with axial dispersion. Radial gradients for mass, velocity and temperature were not considered;
- Uniform packing;
- Internal mass and heat transfer resistances described by a double linear driving force model accounting for the bidisperse porous nature of the adsorbent;
- No temperature gradients inside each particle;
- The column wall only interchanges energy with the gas phase and the external environment.
- Pressure drop locally described by the Ergun equation.

The mass, momentum and energy balance equations of the mathematical model can be found in Table 4; further details can be found elsewhere (da Silva et al. 1999; da Silva and Rodrigues 2001a; Ribeiro et al. 2008).

The transport parameters involved in the model were calculated by commonly used correlations:

- The axial (mass and heat) dispersion coefficients and the mass transfer and heat convective coefficients were estimated using the Wakao and Funazkri correlations (Wakao and Funazkri 1978; Yang 1987; da Silva 1999).
- The convective heat transfer coefficient between the gas and the column wall was calculated with the Wasch and Froment correlation (Wasch and Froment 1972).
- The macropore diffusivity was calculated using the Bosanquet equation and the molecular diffusivities were estimated with the Chapman–Enskog equation (Bird et al. 2002).
- General properties of the gases, i.e. density, viscosity, and molar specific heat were obtained according to Bird et al. (2002). The molar specific heat of the gas in the adsorbed state and gas phase were assumed to be the same (Sircar 1985).

Table 4 Mass, momentum and energy balances of the mathematical model

Mass balances

Gas phase

$$\frac{\partial}{\partial z}\left(\varepsilon D_{ax} C_{g,T} \frac{\partial y_i}{\partial z}\right) - \frac{\partial}{\partial z}\left(u_0 C_{g,i}\right) - \varepsilon \frac{\partial C_{g,i}}{\partial t} - \frac{(1-\varepsilon)\, a_p k_f}{1+Bi_i}\left(C_{g,i} - \overline{C_{p,i}}\right) = 0$$

Solid phase—macropore

$$\frac{\partial \overline{C_{p,i}}}{\partial t} = \frac{15 D_{p,i} Bi_i}{R_p^2 (1+Bi_i)}\left(C_{g,i} - \overline{C_{p,i}}\right) - \frac{\rho_p}{\varepsilon_p}\frac{\partial \overline{q_i}}{\partial t}$$

Solid phase—crystal

$$\frac{\partial \overline{q_i}}{\partial t} = \frac{15 D_{c,i}}{r_c^2}\left(q_i^* - \overline{q_i}\right)$$

Momentum balance

$$-\frac{\partial P}{\partial z} = \frac{150\,\mu(1-\varepsilon)^2}{\varepsilon^3 d_p^2} u_0 + \frac{1.75(1-\varepsilon)\rho}{\varepsilon^3 d_p}|u_0|\, u_0$$

Energy balances

Gas phase

$$\frac{\partial}{\partial z}\left(\lambda \frac{\partial T_g}{\partial z}\right) - u_0 C_{g,T} C_p \frac{\partial T_g}{\partial z} + \varepsilon R_g T_g \frac{\partial C_{g,T}}{\partial t} - (1-\varepsilon)\, a_p\, h_f\, (T_g - T_p) - \frac{4 h_w}{d_{wi}}(T_g - T_w) - \varepsilon C_{g,T} C_V \frac{\partial T_g}{\partial t} = 0$$

Solid phase

$$(1-\varepsilon)\left[\varepsilon_p \sum_{i=1}^{n} \overline{C_{p,i}} C_{v,i} + \rho_p \sum_{i=1}^{n} \overline{q_i} C_{v,ads,i} + \rho_p \hat{C}_{ps}\right]\frac{\partial T_p}{\partial t} = (1-\varepsilon)\,\varepsilon_p R_g T_p \frac{\partial \overline{C_{p,T}}}{\partial t} + \rho_b \sum_{i=1}^{n} (-\Delta H_{ads})_i \frac{\partial \overline{q_i}}{\partial t} + (1-\varepsilon)\, a_p\, h_f\, (T_g - T_p)$$

Column wall

$$\rho_w \hat{C}_{p,w} \frac{\partial T_w}{\partial t} = \alpha_w h_w \left(T_g - T_w\right) - \alpha_{w\ell} U \left(T_w - T_\infty\right)$$

Table 5 Balances to the nodes used in the simulation of SMB

Desorbent node

$$u_{0\,inlet,I}\, C_{inlet,i,I} = u_{0,D}\, C_{D,i} + \left(u_{0,IV}\, C_{g,i,IV}\right)\big|_{z=L_{IV}}$$

$$u_{0\,inlet,I}\, C_{inlet,T,I} = u_{0,D}\, C_{D,T} + \left(u_{0,IV}\, C_{g,T,IV}\right)\big|_{z=L_{IV}}$$

$$u_{0\,inlet,I}\, C_{inlet,T,I}\, C_p\, T_{inlet,I} = u_{0,D}\, C_{D,T}\, C_p\, T_D + \left(u_{0,IV}\, C_{g,T,IV}\, C_p\, T_{g,IV}\right)\big|_{z=L_{IV}}$$

Extract node

$$C_{inlet,i,II} = C_{g,i,I}\big|_{z=L_I}$$

$$u_{0\,inlet,II} = u_{0,I}\big|_{z=L_I} - u_{0,E}$$

$$T_{inlet,II} = T_{g,I}\big|_{z=L_I}$$

Feed node

$$u_{0\,inlet,III}\, C_{inlet,i,III} = u_{0,F}\, C_{F,i} + \left(u_{0,II}\, C_{g,i,II}\right)\big|_{z=L_{II}}$$

$$u_{0\,inlet,III}\, C_{inlet,T,III} = u_{0,F}\, C_{F,T} + \left(u_{0,II}\, C_{g,T,II}\right)\big|_{z=L_{II}}$$

$$u_{0\,inlet,III}\, C_{inlet,T,III}\, C_p\, T_{inlet,III} = u_{0,F}\, C_{F,T}\, C_p\, T_F + \left(u_{0,II}\, C_{g,T,II}\, C_p\, T_{g,II}\right)\big|_{z=L_{II}}$$

Raffinate node

$$C_{inlet,i,IV} = C_{g,i,III}\big|_{z=L_{III}}$$

$$u_{0\,inlet,IV} = u_{0,III}\big|_{z=L_{III}} - u_{0,R}$$

$$T_{inlet,IV} = T_{g,III}\big|_{z=L_{III}}$$

In order to simulate the SMB unit, the mathematical model presented in Table 4 has been complemented with the balances to the nodes presented in Table 5.

The columns were considered to be saturated with desorbent at t = 0. The Danckwerts boundary conditions were considered in the model.

The complete mathematical model used to describe the SMB (presented in Tablea 4 and 5) was implemented in gPROMS® environment v.3.5.1 (Process System Enterprise, London, UK); the problem was numerically solved using orthogonal collocation on finite elements method, with 250 discretization intervals and third order polynomials. The methodology used to calculate the separation region has been described elsewhere by Minceva (2004). In summary, this methodology consists in setting the switching time, and setting γ_I and γ_{IV} with a given tolerance (in this case a tolerance of 2.5 and a switching time of 70 s were used). Then, successive simulations with a low γ_{feed} and increasing γ_{II} values are run until the boundaries of the γ_{II}/γ_{III} separation region that comply with the specified purity requirements are found. Afterwards γ_{feed} is increased in small steps, repeating for each γ_{feed}, the same procedure. Each simulation started with the bed saturated with desorbent and actual SMB operation was run until CSS was achieved.

5 Results and discussion

5.1 Adsorption equilibrium

The dual site Langmuir model was used to fit the experimental adsorption equilibrium values of isobutane over the 13X zeolite adsorbent. This model was also fitted to the adsorption equilibrium data of propane and propylene over this new 13X. The dual site Langmuir model is represented by the following equations:

$$q = q_{m,A}\frac{b_A P}{1+b_A P} + q_{m,B}\frac{b_B P}{1+b_B P} \quad (1)$$

$$b_i = b_{\infty,i}\exp\left(\frac{-\Delta H_i}{R T}\right) \quad i = A, B \quad (2)$$

where A refers to the site A of the dual site Langmuir model and B refers to the site B of the dual site Langmuir model.

The dual site Langmuir model parameters were obtained by minimizing the sum of the absolute error between the

Table 6 Dual site Langmuir parameters for propane, propylene and isobutane adsorption equilibrium isotherms on 13X at 323, 373 and 423 K

	$q_{m,A}$ (mol kg^{-1})	$b_{\infty,A}$ (kPa^{-1})	ΔH_A (kJ mol^{-1})	$q_{m,B}$ (mol kg^{-1})	$b_{\infty,B}$ (kPa^{-1})	ΔH_B (kJ mol^{-1})
Propane[a]	2.49	4.75×10^{-7}	36.15	0.62	4.04×10^{-7}	28.14
Propylene[a]	2.50	6.71×10^{-8}	49.51	0.92	6.98×10^{-10}	50.3
Isobutane[b]	1.82	1.26×10^{-7}	48.47	0.80	1.08×10^{-9}	46.21

[a] Experimental data published elsewhere (Campo et al. 2013)

[b] Experimental data obtained in this work

experimental and the predicted adsorbed amounts, using Excel Solver tool, and are presented in Table 6.

Figure 2 represents the comparison among adsorption isotherms of propane, propylene and isobutane over 13X beads at 323, 373 and 423 K. Propylene adsorption capacity is the highest in the entire pressure and temperature range. Isobutane presents a steep isotherm, showing intermediate adsorption capacities between those of propane and propylene in defined pressure ranges. It is seen that adsorption equilibrium curves of isobutane cross those of propane in the whole temperature range herein studied. At lower pressures, isobutane adsorbs more than propane, reverting this behavior at around 7, 38 and 150 kPa, respectively at 323, 373 and 423 K. Propane presents the lowest heat of adsorption, while propylene and isobutane are similarly sensitive to temperature.

The prediction of multicomponent adsorption equilibrium to be used in the simulations of both fixed bed and SMB was done using the multicomponent extended dual site Langmuir isotherm, given by the following equation:

$$q_k = q_{m,A,k}\frac{b_{A,k}P_k}{1+\sum_{j=1}^{NC} b_{A,j}P_j} + q_{m,B,k}\frac{b_{B,k}P_k}{1+\sum_{j=1}^{NC} b_{B,j}P_j} \quad (3)$$

The parameters obtained in the fitting of the single component equilibrium data (Table 6) were used in prediction of the multicomponent adsorption equilibrium (Eq. 3) without any further "re-fitting".

The saturation capacities are significantly higher than those reported in literature for other shaped zeolite 13X (da Silva and Rodrigues 1999, 2001b). If one compares the adsorption isotherms of propane and propylene on this new

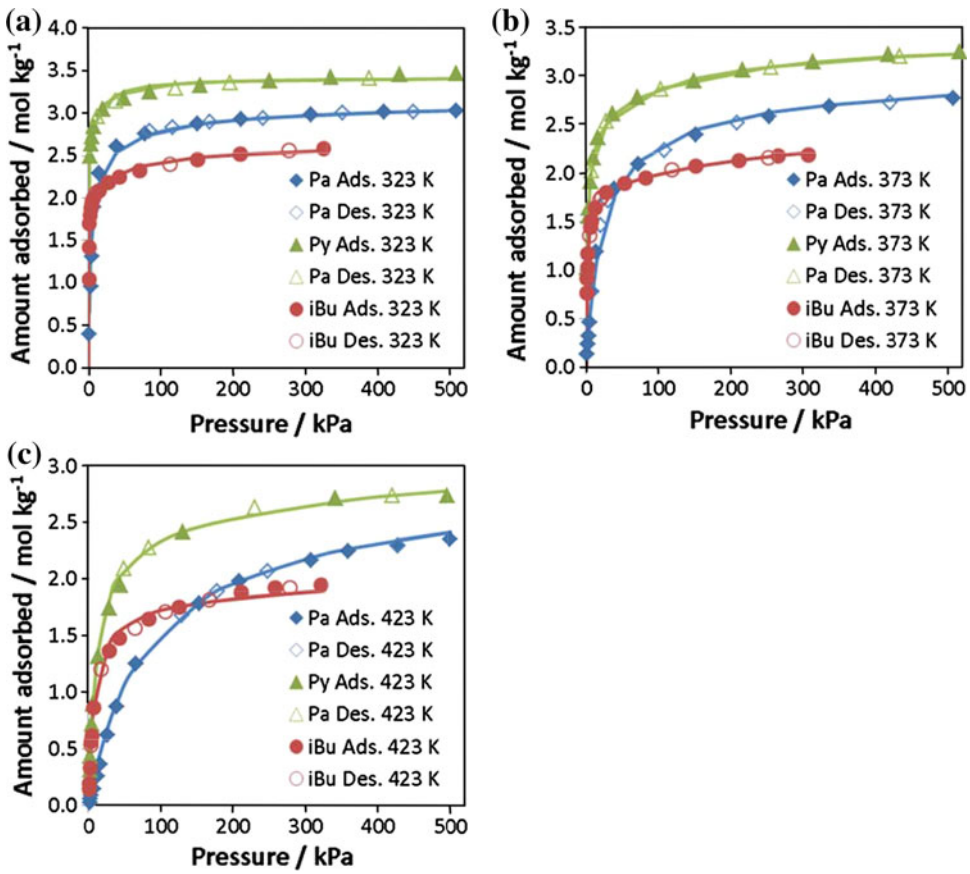

Fig. 2 Adsorption equilibrium isotherms of propane (Campo et al. 2013), propylene (Campo et al. 2013) and isobutane on 13X at 323 K (**a**), 373 K (**b**) and 423 K (**c**). The *points* correspond to experimental points and the *lines* to the dual site Langmuir fitting, respectively (*Pa* propane, *Py* propylene, *iBu* isobutane, *Ads* adsorption branch of the isotherm, and *Des* desorption branch of the isotherm)

shaped 13X zeolite beads, with the isotherms of pure 13X powder it can be verify that the capacity loss corresponds nicely only to the dilution factor of the zeolite with 11 % of inert material (binder).

5.2 Breakthrough curves

Single, pseudo-binary and pseudo-ternary breakthrough curves of isobutane, propane and propylene over shaped 13X zeolite have been determined at 373 K. The fixed-bed mathematical model considering multicomponent non-isothermal adsorption was used to simulate the experimental curves. Experimental and simulation results are shown in Figs. 3, 4, 5 and 6. The adsorption equilibrium parameters used in the model are presented in Table 6.

Single breakthrough curves of propane and propylene over 13X can be found elsewhere (Campo et al. 2013). Single breakthrough curve of isobutane is given in Fig. 3; it presents the adsorption of 1 L_N min^{-1} of isobutane at 373 K and 150 kPa over the same adsorbent.

Isobutane is being adsorbed during the first 490 s; after that, the mass front starts exiting the column and isobutane is detected. Comparing with single propane and propylene breakthrough curves (Campo et al. 2013) at 150 kPa and 373 K, isobutane is the less adsorbed species, leaving therefore, the bed outlet in a time shorter than propane (530 s) and propylene (690 s).

The adsorption capacity calculated from fixed bed experiments (breakthrough curve) is equal to that obtained by the gravimetric method, using the Rubotherm balance for the same temperature and pressure conditions. A temperature peak of about 50 K was observed.

Figure 4b shows the adsorption of isobutane over a bed of 13X zeolite beads initially saturated with propane. This pseudo-binary breakthrough curve is steep and similar to the single isobutane breakthrough case, when the column is initially full with helium; still in Fig. 4b, the respective temperature history indicates an exothermic process, although less pronounced than the adsorption of isobutane over helium; the heat released during the adsorption of isobutane is greater than the heat consumed by propane desorption. In the reverse case, i.e. adsorption of propane over a bed initially filled with isobutane (Fig. 4a), the curves present more dispersion. Experimentally, the temperature history indicates an isothermal process, which means that the heat released from propane adsorption is compensating the heat consumed during isobutane desorption.

Simulation results indicate a good prediction for isobutane adsorption and propane displacement, failing a little

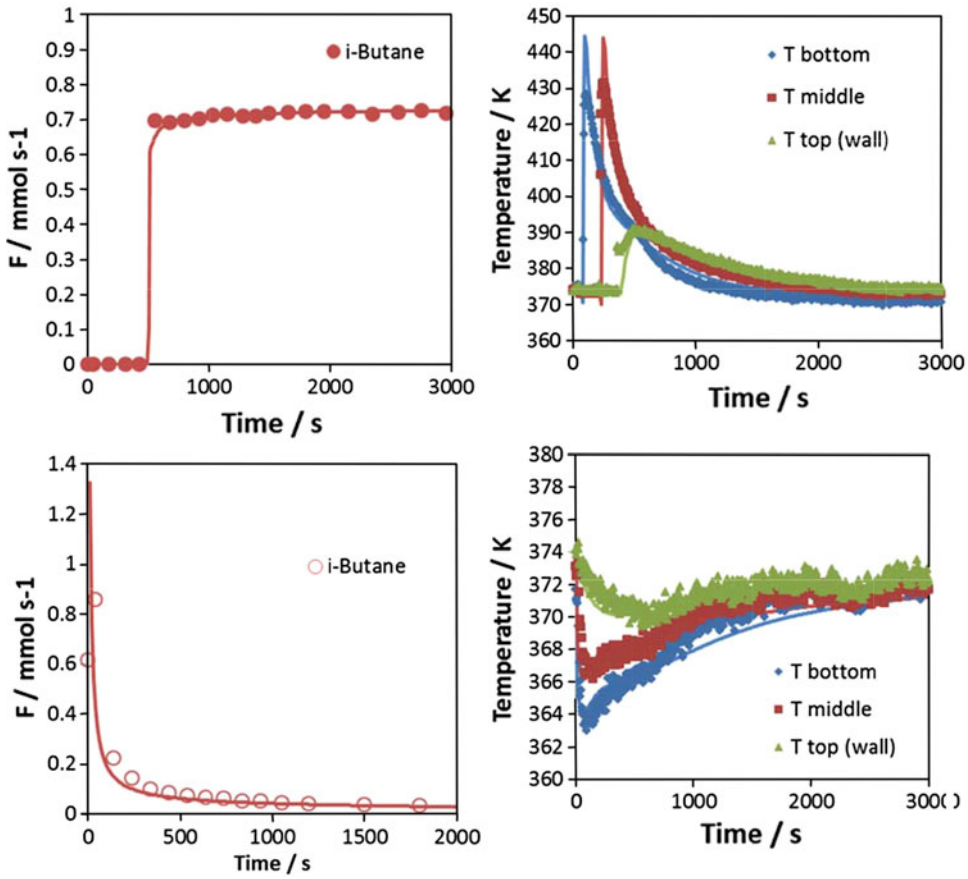

Fig. 3 Adsorption of isobutane over 13X (bed initially full with helium) and desorption in helium flow at 150 kPa and 373 K (feed flowrate: 1 L_N min^{-1}) (*left*); temperature histories inside the bed (*right*). The *lines* are simulation results

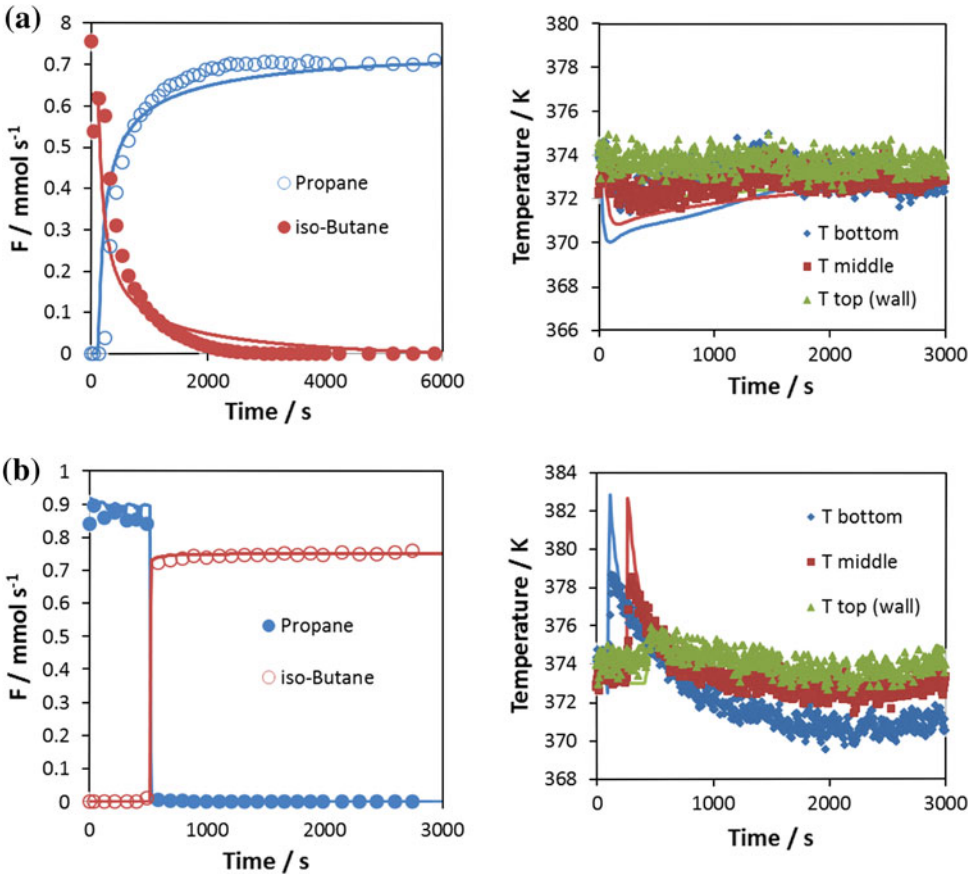

Fig. 4 Pseudobinary breakthrough curve over 13X zeolite: **a** Adsorption of 1 L_N min^{-1} of propane over a bed initially full of isobutane at 373 K, 150 kPa; **b** adsorption of 1 L_N min^{-1} of isobutane over a bed initially full of propane at 373 K, 150 kPa. *Right* molar flow rate at the column outlet; *left* temperature histories. The *lines* are simulation results

bit in the reverse case. However, generally, it describes the whole picture in a reasonable way.

Figure 5a presents the adsorption of pure propylene over a bed initially saturated with isobutane, with an exothermic temperature history. Figure 5b shows the reverse case, where isobutane is adsorbed over a bed saturated with propylene. In both cases, each species is able of displacing the other, easily, as required for SMB operation.

The term pseudo-ternary breakthrough curve refers to the adsorption of a binary mixture of propane and propylene (25:75) over a bed initially saturated with isobutane, and the other way round, where the mixture is displaced by isobutane.

The pseudo-ternary breakthrough curve shown in Fig. 6 represents the adsorption of a mixture of 75 % propylene and 25 % propane over a bed initially saturated with isobutane (a); isobutane is displaced by the problem mixture. First, all the propylene is adsorbed and only propane (less adsorbable product) and isobutane exit the bed. Then propylene breaks through, and the outlet concentrations tend to meet those of the feed.

Figure 6b shows the displacement of the propane/propylene mixture by the desorbent. It can be seen that this step, essential for continuous SMB operation, is also feasible. Propane and propylene are easily desorbed by isobutane. Nevertheless propylene presents though a more tailing desorption curve than propane.

Again, the mathematical model proposed before is reasonably predicting experimental data, even for this three-component system.

5.3 SMB technology to produce polymer grade propylene

The complete dynamic model previously proposed and validated through experimental breakthrough curves has been used to simulate a gas phase SMB unit capable of producing polymer grade propylene (99.5 % minimum propylene purity) from a mixture of 25 % propane/75 % propylene at 373 K, and 150 kPa.

The definitions of the purity of the extract and raffinate, in terms of the discontinuous SMB model can be obtained from the average values for a switching period or over a complete cycle period ($N_c t_s$), as follows:

Purity of extract and raffinate

$$Pu^{X}_{C_3H_6}(\%) = \frac{\int_t^{t+N_c t_s} C^{X}_{C_3H_6} dt}{\int_t^{t+N_c t_s} \left(C^{X}_{C_3H_6} + C^{X}_{C_3H_8} \right) dt} \times 100 \quad (4)$$

$$Pu^{R}_{C_3H_8}(\%) = \frac{\int_t^{t+N_c t_s} C^{R}_{C_3H_8} dt}{\int_t^{t+N_c t_s} \left(C^{R}_{C_3H_6} + C^{R}_{C_3H_8} \right) dt} \times 100 \quad (5)$$

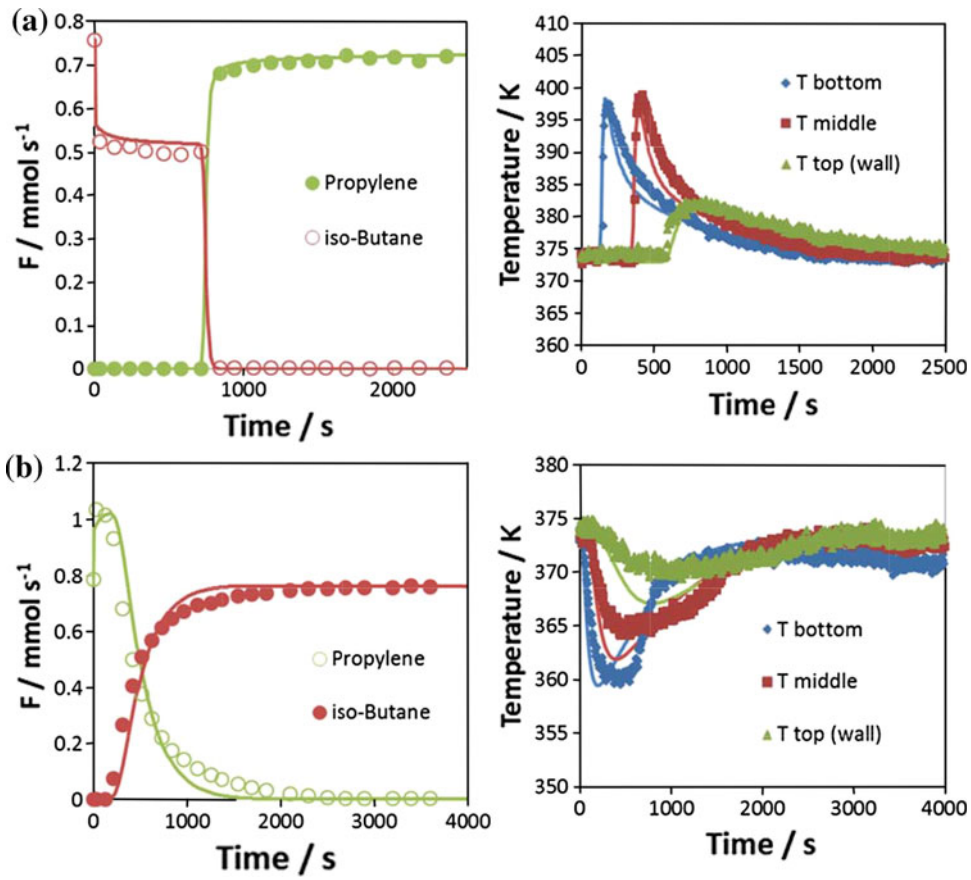

Fig. 5 Pseudobinary breakthrough curve over 13X: **a** Adsorption of 1 L_N min^{-1} of propylene over a bed initially full of isobutane at 373 K, 150 kPa; **b** adsorption of 1 L_N min^{-1} of isobutane over a bed initially full of propylene at 373 K, 150 kPa. *Right* molar flow rate at the column outlet; *left* temperature histories. The *lines* are simulation results

Recovery of extract and raffinate

$$Rec^{X}_{C_3H_6}(\%) = \frac{Q_X \int_t^{t+N_c t_s} C^{X}_{C_3H_6} dt}{Q_F C^{F}_{C_3H_6} N_c t_s} \times 100 \quad (6)$$

$$Rec^{R}_{C_3H_8}(\%) = \frac{Q_X \int_t^{t+N_c t_s} C^{R}_{C_3H_8} dt}{Q_F C^{F}_{C_3H_8} N_c t_s} \times 100 \quad (7)$$

Productivity of extract and raffinate

$$Pro^{X}_{C_3H_6} = \frac{Q_x \int_t^{t+N_c t_s} C^{X}_{C_3H_6} dt}{V_{ads} N_c t_s} = \frac{Rec^{X}_{C_3H_6} Q_F C^{X}_{C_3H_6}}{V_{ads}} \quad (8)$$

$$Pro^{R}_{C_3H_8} = \frac{Q_R \int_t^{t+N_c t_s} C^{R}_{C_3H_8} dt}{V_{ads} N_c t_s} = \frac{Rec^{R}_{C_3H_8} Q_F C^{R}_{C_3H_8}}{V_{ads}} \quad (9)$$

The separation region with a 2–2–2–2 configuration was determined, for product purity values in the extract outlet over 99.5 % (C_3H_6 rich stream, desorbent free basis) and raffinate outlet over 96.5 % (C_3H_8 rich stream, desorbent free basis), as defined by Grande et al. (2010b). The results obtained are show in Fig. 7. The transport parameters used in the simulations of the gas phase SMB are presented in Table 7. γ_{II} and γ_{III} represent the ratio between the fluid and solid interstitial velocities in sections II and III, respectively.

$$\gamma_i = \frac{u_i}{u_s} \quad (10)$$

The equivalency between SMB and TMB dictates that the solid velocity, u_s, is given by $u_s = L/t_s$. The flowrates of eluent and recycle were calculated using a tolerance factor of 2.5, i.e., $\gamma_I = 2.5 \times \gamma_{I,\min}$ and $\gamma_{IV} = \frac{\gamma_{IV,\max}}{2.5}$.

The operating and performance parameters obtained for five points marked with black crosses (A–E) in Fig. 7 are given in Table 8.

It can be seen that for the three points located within the separation region (A–C) the purity and recovery of both products (desorbent free basis) are very high, around 99.9 %. Regarding productivity, the higher value is obtained for point A, as it is closer to the optimum operating point near the vertice of the separation region (higher feed). For the two points located outside the separation region, only one product is obtained at high purity, high propylene purity (extract) for point D and high propane purity (raffinate) for point E.

Figure 8 shows the gas phase concentration, gas phase temperature, total pressure and fluid superficial velocity profiles obtained at CSS 35 s before the switch for point A of Fig. 7.

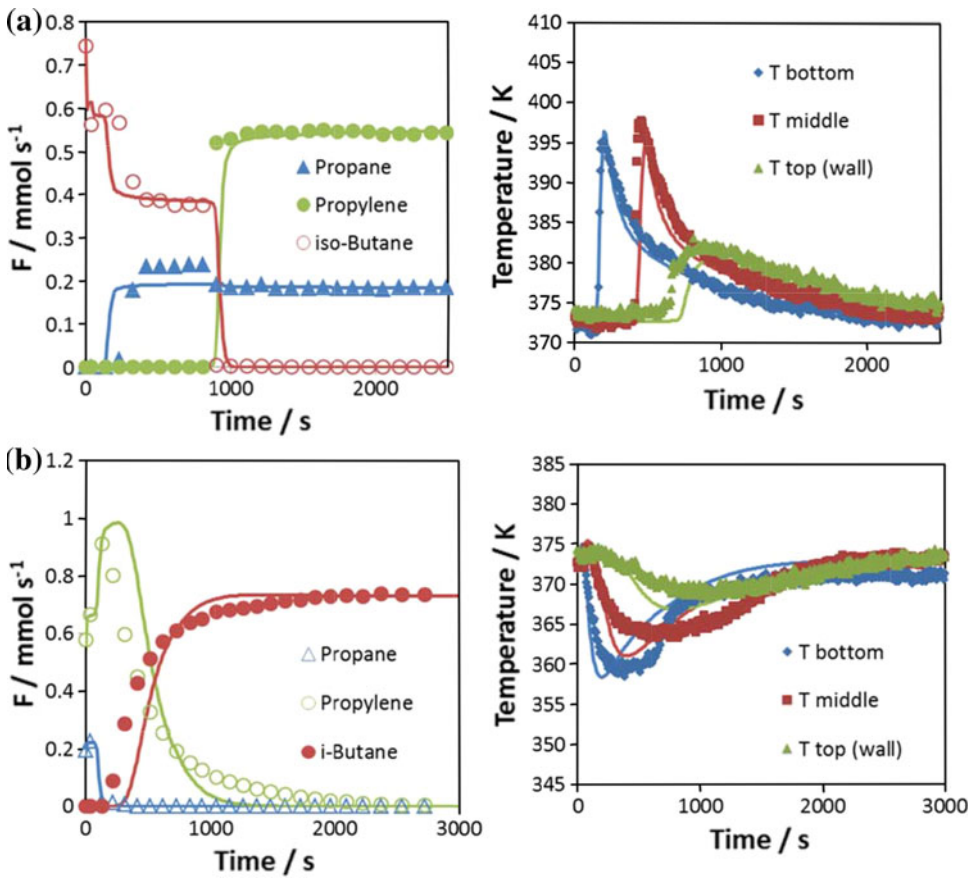

Fig. 6 Isobutane/propane–propylene pseudo-ternary breakthrough curve over 13X at 150 kPa and 373 K: **a** Adsorption of 1 L_N min^{-1} of a binary mixture with 25 % propane and 75 % propylene over a bed initially saturated with isobutane; **b** desorption with 1 L_N min^{-1} of isobutane over a bed initially saturated with a binary mixture of 25 % propane and 75 % propylene. *Right* molar flow rate at the column outlet; *left* temperature histories. The *lines* are simulation results

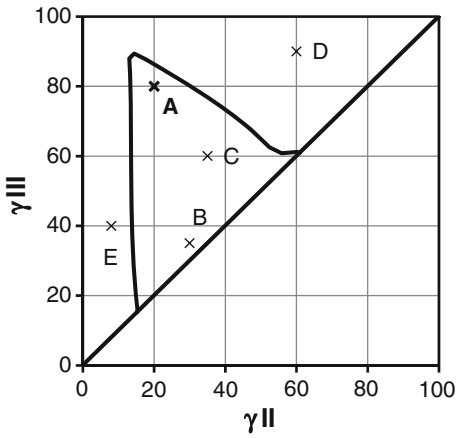

Fig. 7 Separation region determined with the complete model for 150 kPa and 373 K, 8 beds with configuration 2–2–2–2, for purity values in the extract outlet over 99.5 % and raffinate outlet over 96.5 %

Table 7 Transport parameter values used in the simulations at feed conditions (373 K and 150 kPa)

D_{ax} (m^2 s^{-1})	2.9×10^{-4}
λ (J s^{-1} m^{-1} K^{-1})	0.21
k_f (m s^{-1})	0.05
h_f (W m^{-2} K^{-1})	160
h_w (W m^{-2} K^{-1})	40
U (W m^{-2} K^{-1})	20
D_p (m^2 s^{-1})	C_3H_8: 2.84×10^{-6}
	C_3H_6: 2.84×10^{-6}
	C_4H_{10}: 2.39×10^{-6}
D_c (m^2 s^{-1})	C_3H_8: 3.31×10^{-11}
	C_3H_6: 4.20×10^{-11}
	C_4H_{10}: 4.42×10^{-11}

The feed stream is introduced in the node located between section II and III. It can be seen that the propylene concentration decreases in section III and that only propane moves forward to the raffinate node (between sections III and IV). In section IV, the concentration of propane decreases and a pure isobutane stream is obtained at the end of the section to be recycled to section I. On the other hand, the propane concentration decreases in section II, and a pure propylene stream is obtained in the extract node (between sections I and II). In section I, the propylene concentration decreases and regenerated adsorbent is obtained in section IV.

The temperature variations along the system are 30 K. The pressure drop is small, being more important in section I where the fluid velocity is higher. The variation in the fluid velocities between sections can be seen in Fig. 8c due

Table 8 Operating and performance parameters obtained for the selected operation points

A	Q_{Feed} (L_N min^{-1})	Q_{Eluent} (L_N min^{-1})	$Q_{Extract}$ (L_N min^{-1})	$Q_{Raffinate}$ (L_N min^{-1})	$Q_{Recycle}$ (L_N min^{-1})	t_s (s)
	0.91	1.82	1.58	1.15	0.08	70
	Extract—C_3H_6			Raffinate—C_3H_8		
	Purity (%)	Recovery (%)	Productivity (mol kg_{ads}^{-1} h^{-1})	Purity (%)	Recovery (%)	Productivity (mol kg_{ads}^{-1} h^{-1})
	99.996	99.964	17.632	99.892	99.988	5.879
B	Q_{Feed} (L_N min^{-1})	Q_{Eluent} (L_N min^{-1})	$Q_{Extract}$ (L_N min^{-1})	$Q_{Raffinate}$ (L_N min^{-1})	$Q_{Recycle}$ (L_N min^{-1})	t_s (s)
	0.08	1.82	1.43	0.47	0.08	70
	Extract—C_3H_6			Raffinate—C_3H_8		
	Purity (%)	Recovery (%)	Productivity (mol kg_{ads}^{-1} h^{-1})	Purity (%)	Recovery (%)	Productivity (mol kg_{ads}^{-1} h^{-1})
	99.997	99.999	1.459	99.999	99.990	0.486
C	Q_{Feed} (L_N min^{-1})	Q_{Eluent} (L_N min^{-1})	$Q_{Extract}$ (L_N min^{-1})	$Q_{Raffinate}$ (L_N min^{-1})	$Q_{Recycle}$ (L_N min^{-1})	t_s (s)
	0.38	1.82	1.35	0.85	0.08	70
	Extract—C_3H_6			Raffinate—C_3H_8		
	Purity (%)	Recovery (%)	Productivity (mol kg_{ads}^{-1} h^{-1})	Purity (%)	Recovery (%)	Productivity (mol kg_{ads}^{-1} h^{-1})
	99.997	99.998	7.347	99.995	99.999	2.449
D	Q_{Feed} (L_N min^{-1})	Q_{Eluent} (L_N min^{-1})	$Q_{Extract}$ (L_N min^{-1})	$Q_{Raffinate}$ (L_N min^{-1})	$Q_{Recycle}$ (L_N min^{-1})	t_s (s)
	0.45	1.82	0.97	1.30	0.08	70
	Extract—C_3H_6			Raffinate—C_3H_8		
	Purity (%)	Recovery (%)	Productivity (mol kg_{ads}^{-1} h^{-1})	Purity (%)	Recovery (%)	Productivity (mol kg_{ads}^{-1} h^{-1})
	99.994	18.922	1.671	29.134	99.996	2.944
E	Q_{Feed} (L_N min^{-1})	Q_{Eluent} (L_N min^{-1})	$Q_{Extract}$ (L_N min^{-1})	$Q_{Raffinate}$ (L_N min^{-1})	$Q_{Recycle}$ (L_N min^{-1})	t_s (s)
	0.48	1.82	1.76	0.54	0.08	70
	Extract—C_3H_6			Raffinate—C_3H_8		
	Purity (%)	Recovery (%)	Productivity (mol kg_{ads}^{-1} h^{-1})	Purity (%)	Recovery (%)	Productivity (mol kg_{ads}^{-1} h^{-1})
	93.966	99.999	9.406	93.966	80.736	2.531

to the introduction or removal of the different streams in the nodes.

For this point (A), the obtained purity for propylene was 99.996 and 99.892 % for propane; the recovery was 99.964 % for propylene and 99.988 % for propane. The productivity achieved with this adsorbent was 17.632 $mol_{C_3H_6}$ kg^{-1} h^{-1} and 5.879 $mol_{C_3H_8}$ kg^{-1} h^{-1}.

In order to compare the performance of this adsorbent with a conventional commercial 13X zeolite, a similar procedure of simulating an SMB unit for the production of polymer grade propylene has been done. Adsorption equilibrium data for the equivalent propane/propylene/isobutane system was reported by Lamia et al. (Lamia et al. 2007; Gomes et al. 2009) and has been used to recalculate the performance of a similar SMB unit. The results have shown that the new and improved 13X zeolite beads studied in this paper, led to productivity gains of around 25 %, with half desorbent consumption, when compared to a commercial 13X. The improved performance is mainly due to smaller mass transfer resistances (5.2 times lower). The particle diameter of this new material is less than half (0.7 vs. 1.6 mm) than the commercial material studied by Lamia et al. (2007) and Gomes et al. (2009).

6 Conclusions

A gas phase SMB technology using an improved 13X zeolite adsorbent and isobutane as desorbent was considered for the separation of propane/propylene. Adsorption equilibrium of the desorbent isobutane was experimentally determined and modeled using dual site Langmuir

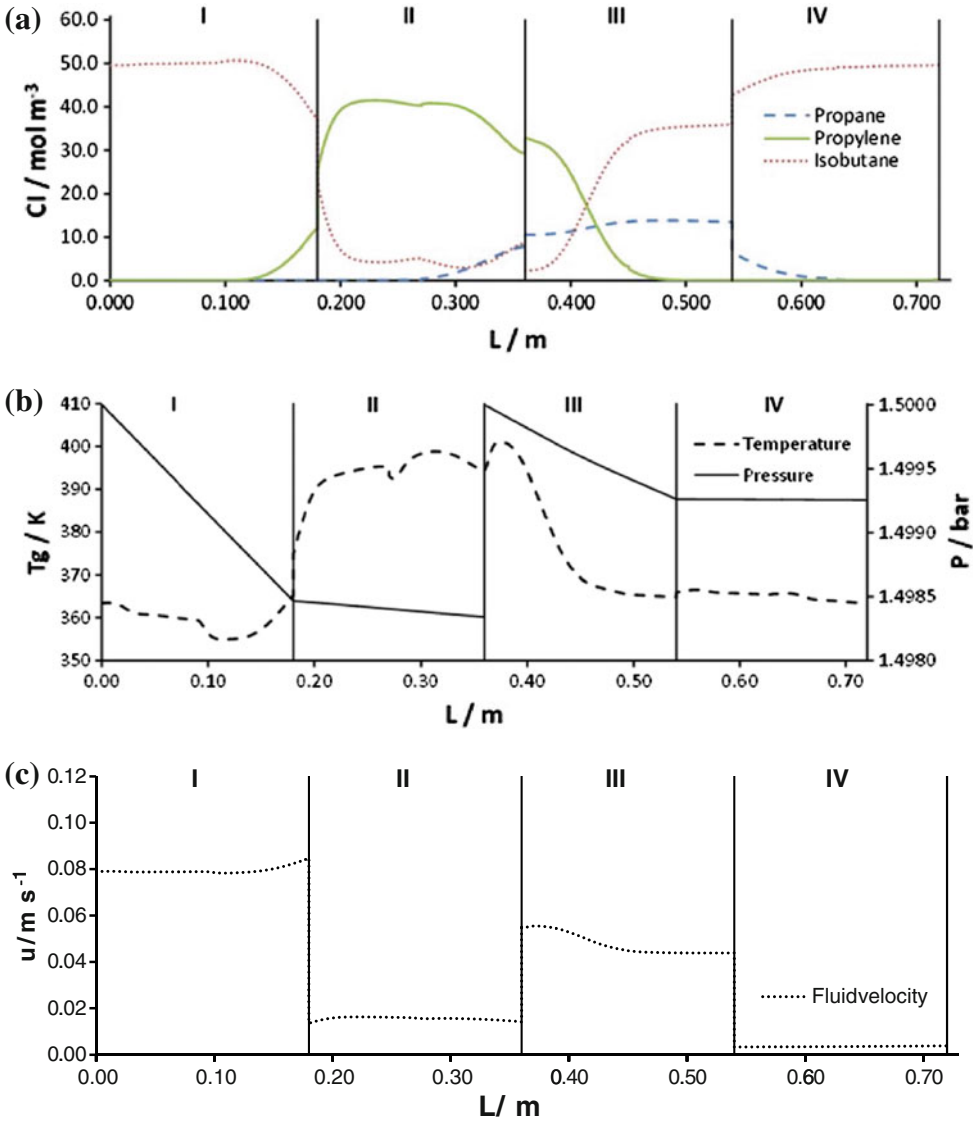

Fig. 8 Profiles obtained at the middle of the step for the selected operation point (configuration 2–2–2–2): **a** Gas phase concentration; **b** gas phase temperature and total pressure; **c** fluid superficial velocity

equation. Furthermore, single and combined breakthrough curves involving propane, propylene and isobutane were experimentally determined, in order to validate the mathematical model herein proposed to describe the dynamics of the system. Finally, and using the previously mentioned model, the simulation of the SMB unit with a feed stream of 75 % propylene in propane revealed that the 99.5 % (in propylene) separation region is possible to achieve. The results obtained for the operation point A within the 99.5 % separation region were: propylene purity and recovery of, respectively, 99.9 and 99.9 % with a productivity of 17.6 $mol_{C_3H_6}$ kg^{-1} h^{-1}; and propane purity and recovery of, respectively, 99.8 and 99.9 % with a productivity of 5.8 $mol_{C_3H_8}$ kg^{-1} h^{-1}. Due to the enhanced capacities of this improved 13X zeolite and small particle size, the productivity of the process was improved 25 % when compared to a commercial 13X (Lamia et al. 2007), and with a half eluent consumption.

Acknowledgments This work is partially supported by project PEst-C/EQB/LA0020/2011, financed by FEDER through COMPETE—Programa Operacional Factores de Competitividade and by FCT—Fundação para a Ciência e a Tecnologia. The authors are also thankful to the FCT funding provided in the framework of the project "Eco-efficient Separation of Propane/Propylene by Gas Phase Simulated Moving Bed" with reference PTDC/EQU–EQU/103756/2008. The authors acknowledge CECA for providing the zeolite 13X.

References

Abe, T., Tanzawa, S., Takayuki, M.: Method and apparatus for separating, removing, and recovering gas components. U.S. Patent 6.461.410 (2002)

Aitani, A.M.: Propylene production. In: Lee, S. (ed.) Encyclopedia of Chemical Processing, pp. 2461–2466. Taylor & Francis, New York (2006)

Baciocchi, R., Mazzotti, M., Storti, G., Morbidelli, M.: C-5 separation in a vapor phase simulated moving bed unit. Kluwer Int. Ser. Eng. C **356**, 75–82 (1996)

Bird, R.B., Stewart, W.E., Lightfoot, E.N.: Transport Phenomena, 2nd edn. Wiley International, Singapore (2002)

Broughton, D.B., Gerhold, C.G.: Continuous sorption process employing fixed bed of sorbent and moving inlets and outlets. U.S. Patent 2985589 (1961)

Bryan, P.F.: Removal of propylene from fuel-grade propane. Sep. Purif. Rev. **33**(2), 157–182 (2004)

Campo, M.C., Ribeiro, A.M., Ferreira, A.F.P., Santos, J.C., Lutz, C., Loureiro, J.M., Rodrigues, A.E.: New 13X zeolite for propylene/propane separation by VSA. Sep. Purif. Technol. **103**, 60–70 (2013)

CHEMSYSTEMS: Evolving Propylene Sources—Solution to Supply Shortages? Nexant, Inc., White Plains (2012)

Chen, J.P., Yang, R.T.: A molecular orbital study of the selective adsorption of simple hydrocarbon molecules on Ag+- and Cu+-exchanged resins and cuprous halides. Langmuir **11**(9), 3450–3456 (1995)

Cheng, L.S., Wilson, S.T.: Process for separating propylene from propane. U.S. Patent 6293999 B1 (2001a)

Cheng, L.S., Wilson, S.T.: Vacuum swing adsorption process for separating propylene from propane. U.S. Patent 6296688 (2001b)

da Silva, F.A.: Cyclic Adsorption Processes: Application to Propane/Propylene Separation. University of Porto, Porto (1999)

da Silva, F.A., Rodrigues, A.E.: Adsorption equilibria and kinetics for propylene and propane over 13X and 4A zeolite pellets. Ind. Eng. Chem. Res. **38**(5), 2051–2057 (1999)

da Silva, F.A., Silva, J.A., Rodrigues, A.E.: A general package for the simulation of cyclic adsorption processes. Adsorption **5**(3), 229–244 (1999)

da Silva, F.A., Rodrigues, A.E.: Vacuum swing adsorption for propylene/propane separation with 4A zeolite. Ind. Eng. Chem. Res. **40**(24), 5758–5774 (2001a)

da Silva, F.A., Rodrigues, A.E.: Propylene/propane separation by vacuum swing adsorption using 13X zeolite. AIChE J. **47**(2), 341–357 (2001b)

Ferreira, A.F.P., Santos, J.C., Plaza, M.G., Lamia, N., Loureiro, J.M., Rodrigues, A.E.: Suitability of Cu-BTC extrudates for propane–propylene separation by adsorption processes. Chem. Eng. J. **167**(1), 1–12 (2011)

GBI-Research: Polypropylene Market to 2020—Propylene Supply Shortages to Restrict Industry Expansion. GBI Research (2010)

Ghosh, T. K., Lin, H.-D., Hines, A.L.: Hybrid adsorption–distillation process for separating propane and propylene. Ind. Eng. Chem. Res. **32**, 2390–2399 (1993)

Gomes, P.S., Lamia, N., Rodrigues, A.E.: Design of a gas phase simulated moving bed for propane/propylene separation. Chem. Eng. Sci. **64**(6), 1336–1357 (2009)

Granato, M.A., Vlugt, T.J.H., Rodrigues, A.E.: Potential desorbents for propane/propylene separation by gas phase simulated moving bed: a molecular simulation study. Ind. Eng. Chem. Res. **49**(12), 5826–5833 (2010)

Grande, C.A., Cavenati, S., Da Silva, F.A., Rodrigues, A.E.: Carbon molecular sieves for hydrocarbon separations by adsorption. Ind. Eng. Chem. Res. **44**(18), 7218–7227 (2005)

Grande, C.A., Gascon, J., Kapteijn, F., Rodrigues, A.E.: Propane/propylene separation with Li-exchanged zeolite 13X. Chem. Eng. J. **160**(1), 207–214 (2010a)

Grande, C.A., Poplow, F., Rodrigues, A.E.: Vacuum pressure swing adsorption to produce polymer-grade propylene. Sep. Sci. Technol. **45**, 1252–1259 (2010b)

Jarvelin, H., Fair, J.R.: Adsorptive separation of propylene–propane mixtures. Ind. Eng. Chem. Res. **32**(10), 2201–2207 (1993)

Johannsen, M.: Modeling of simulated moving-bed chromatography. In: Keil, F.J. (ed.) Modeling of Process Intensification. Wiley-VCH, Weinheim (2007)

Jorge, M., Lamia, N., Rodrigues, A.E.: Molecular simulation of propane/propylene separation on the metal–organic framework CuBTC. Colloids Surf. A **357**(1–3), 27–34 (2010)

Kostroski, K.P., Wankat, P.C.: Separation of dilute binary gases by simulated-moving bed with pressure-swing assist: SMB/PSA processes. Ind. Eng. Chem. Res. **47**(9), 3138–3149 (2008)

Lamia, N., Wolff, L., Leflaive, P., Gomes, P.S., Grande, C.A., Rodrigues, A.E.: Propane/propylene separation by simulated moving bed I. Adsorption of propane, propylene and isobutane in pellets of 13X zeolite. Sep. Sci. Technol. **42**(12), 2539–2566 (2007)

Lamia, N.: Modélisation de la Séparation du Mélange Propane/Propylène par Adsorption en Lit Mobile Simulé. Ph.D. thesis, University of Porto (2008)

Lamia, N., Wolff, L., Leflaive, P., Leinekugel-Le-Cocq, D., Gomes, P.S., Grande, C.A., Rodrigues, A.E.: Equilibrium and fixed bed adsorption of 1-butene, propylene and propane over 13X zeolite pellets. Sep. Sci. Technol. **43**(5), 1124–1156 (2008)

Lamia, N., Jorge, M., Granato, M.A., Almeida Paz, F.A., Chevreau, H., Rodrigues, A.E.: Adsorption of propane, propylene and isobutane on a metal-organic framework: molecular simulation and experiment. Chem. Eng. Sci. **64**(14), 3246–3259 (2009)

Mazzotti, M., Baciocchi, R., Storti, G., Morbidelli, M.: Vapor-phase SMB adsorptive separation of linear/nonlinear paraffins. Ind. Eng. Chem. Res. **35**(7), 2313–2321 (1996)

Minceva, M.: Separation/isomerization of xylenes by simulated moving bed technology. Ph.D thesis, University of Porto (2004)

Mota, J.P.B., Esteves, I.A.A.C.: Optimal design and experimental assessment of time-variable simulated moving bed for gas separation. Ind. Eng. Chem. Res. **46**(21), 6978–6988 (2007)

Mota, J.P.B., Esteves, I.A.A.C., Eusbio, M.F.J.: Synchronous and asynchronous SMB processes for gas separation. AIChE J. **53**(5), 1192–1203 (2007)

Plaza, M.G., Ferreira, A.F.P., Santos, J.C., Ribeiro, A.M., Müller, U., Trukhan, N., Loureiro, J.M., Rodrigues, A.E.: Propane/propylene separation by adsorption using shaped copper trimesate MOF. Microporous Mesoporous Mater. **157**, 101–111 (2012a)

Plaza, M.G., Ribeiro, A.M., Ferreira, A., Santos, J.C., Hwang, Y.K., Seo, Y.K., Lee, U.H., Chang, J.S., Loureiro, J.M., Rodrigues, A.E.: Separation of C3/C4 hydrocarbon mixtures by adsorption using a mesoporous iron MOF: MIL-100(Fe). Microporous Mesoporous Mater. **153**, 178–190 (2012b)

Rao, D.P., Sivakumar, S.V., Mandal, S., Kota, S., Ramaprasad, B.S.G.: Novel simulated moving-bed adsorber for the fractionation of gas mixtures. J. Chromatogr. A **1069**(1), 141–151 (2005)

Rege, S.U., Padin, J., Yang, R.T.: Olefin/paraffin separations by adsorption: π-complexation vs kinetic separation. AIChE J. **44**(4), 799–809 (1998)

Rege, S.U., Yang, R.T.: Propane/propylene separation by pressure swing adsorption: sorbent comparison and multiplicity of cyclic steady states. Chem. Eng. Sci. **57**(7), 1139–1149 (2002)

Ribeiro, A.M., Grande, C.A., Lopes, F.V.S., Loureiro, J.M., Rodrigues, A.E.: A parametric study of layered bed PSA for hydrogen purification. Chem. Eng. Sci. **63**, 5258–5273 (2008)

Rodrigues, A.E., Lamia, N., Grande, C.A., Wolff, L., Leflaive, P., Leinekugel-le-Coq, D.: Procédé de Séparation du Propylène en Mélange avec du Propane par Adsorption en Lit Mobile Simulé en Phase Gaz ou Liquide utilisant une Zéolithe de type Faujasite 13X comme Solide Adsorbant. FR. Patent 2,903,981 A1 (2006) and WO Patent 2008/012410 A1 (2008)

Rothchild, R.D.: Gas separation by continuous pressure-swing chromatography. U.S. Patent 5.672.197 (2001)

Ruthven, D.M., Ching, C.B.: Countercurrent and simulated countercurrent adsorption separation processes. Chem. Eng. Sci. **44**(5), 1011–1038 (1989)

Ruthven, D.M., Reyes, S.C.: Adsorptive separation of light olefins from paraffins. Microporous Mesoporous Mater. **104**(1–3), 59–66 (2007)

Sircar, S.: Excess properties and thermodynamics of multicomponent gas adsorption. J. Chem. Soc. Faraday Trans. **81**, 1527–1540 (1985)

Storti, G., Mazzotti, M., Furlan, L.T., Morbidelli, M., Carra, S.: Performance of a 6-port simulated moving-bed pilot-plant for vapor-phase adsorption separations. Sep. Sci. Technol. **27**(14), 1889–1916 (1992)

van den Bergh, J., Gücüyener, C., Pidko, E.A., Hensen, E.J.M., Gascon, J., Kapteijn, F.: Understanding the anomalous alkane selectivity of ZIF-7 in the separation of light alkane/alkene mixtures. Chem. A Eur. J. **17**(32), 8832–8840 (2011)

Wagener, A., Rudolphi, F., Schindler, M., Ernst, S.: Trennung von propan/propen-gemischen durch adsorption an metallorganischen koordinationspolymeren. Chem. Ing. Tech. **78**(9), 1328–1329 (2006)

Wagener, A., Schindler, M., Rudolphi, F., Ernst, S.: Metallorganische Koordinationspolymere zur Adsorptiven Trennung von Propan/Propen-Gemischen. Chem. Ing. Tech. **79**(6), 851–855 (2007)

Wakao, N., Funazkri, T.: Effect of fluid dispersion coefficients on particle-to-fluid mass transfer coefficients in packed beds. Chem. Eng. Sci. **33**(10), 1375–1384 (1978)

Wasch, A.P.D., Froment, G.F.: Heat transfer in packed beds. Chem. Eng. Sci. **27**, 567–576 (1972)

Yang, R.T.: Gas Separation by Adsorption Processes. Butterworths, Boston (1987)

Yoon, J., Seo, Y.K., Hwang, Y., Chang, J.S., Leclerc, H., Wuttke, S., Bazin, P., Vimont, A., Daturi, M., Bloch, E., Llewellyn, P., Serre, C., Horcajada, P., Grenèche, J.M., Rodrigues, A., Férey, G.: Controlled reducibility of a metal–organic framework with coordinatively unsaturated sites for preferential gas sorption. Angew. Chem. Int. Ed. **49**(34), 5949–5952 (2010a)

Yoon, J.W., Jang, I.T., Lee, K.-Y., Hwang, Y.K., Chang, J.-S.: Adsorptive separation of propylene and propane on a porous metal-organic framework, copper trimesate. Bull. Korean Chem. Soc. **31**(1), 220–223 (2010b)

Zhu, W., Kapteijn, F., A. Moulijn, J.: Shape selectivity in the adsorption of propane/propene on the all-silica DD3R. Chem. Commun. **24**, 2453–2454 (1999)